CHEMISTRY OF MATERIALS
Cite This: Chem. Mater. 2018, 30, 309−313
Communication
pubs.acs.org/cm

Panchromatic Ternary Photovoltaic Cells Using a Nonfullerene Acceptor Synthesized Using C−H Functionalization

Junxiang Zhang,[†,#] Cenqi Yan,[‡,#] Wei Wang,[‡] Yiqun Xiao,[⊥] Xinhui Lu,[⊥] Stephen Barlow,[†] Timothy C. Parker,[†] Xiaowei Zhan,[*,‡] and Seth R. Marder[*,†]

[†]Center for Organic Photonics and Electronics, and School of Chemistry and Biochemistry, Georgia Institute of Technology, Atlanta, Georgia 30332-0400, United States

[‡]Department of Materials Science and Engineering, College of Engineering, Key Laboratory of Polymer Chemistry and Physics of Ministry of Education, Peking University, Beijing 100871, China

[⊥]Department of Physics, The Chinese University of Hong Kong, New Territories, Hong Kong, China

Supporting Information

Downloaded via SYNCHROTRON RADIATION RESEARCH on January 21, 2019 at 04:16:33 (UTC).
See https://pubs.acs.org/sharingguidelines for options on how to legitimately share published articles.

Some of the most significant recent advances in organic solar cells (OSCs) have been in developing nonfullerene acceptors (NFAs),[1−7] potential advantages of which over fullerenes include easier and lower cost synthesis and purification, stronger absorption, and easier tunability of absorption bands and electron affinities (EAs) via structural changes.[8,9] Indacenodithiophene (IDT)-based NFAs have attracted particular interest, owing to their high electron mobilities (comparable to or exceeding those of fullerenes) and strong absorption at ca. 600−800 nm.[10,11] To complement their absorption in bulk heterojunction blends, wide- or medium-bandgap polymers are usually chosen as donors.[12] However, to exploit the low-bandgap donor polymers extensively developed for use with fullerenes, NFAs with even lower bandgaps in the near-infrared (NIR) are desirable. IHIC (Figure 1),[13] in which the central arene of IDT derivatives is replaced with thienothiophene, was recently reported as a NIR-absorbing NFA. OSCs based on binary blends of IHIC with PTB7-Th (Figure 1) show high power conversion efficiency (PCE) of 9.77%.

To increase the PCE of PTB7-Th:IHIC OSCs, we were inspired by recent reports of OSCs using ternary blends of a donor polymer with two acceptors.[14−17] The third component should ideally: (i) have an EA lower than that of IHIC, in order to avoid compromising V_{OC}, but still sufficiently large to accept an electron from photoexcited PTB7-Th; and (ii) absorb at higher energy than IHIC and PTB7-Th and/or significantly more strongly than PTB7-Th in order to afford a more panchromatic absorption and higher short-circuit current density (J_{SC}). Here we report a new NFA, IHIC-N (Figure 1), in which a naphthalene core is chosen to provide a higher π-surface area than that of IDT to potentially interact more strongly with the polymer π-system. The synthesis of a key intermediate is enabled by a double carboxylate-directed C−H bond functionalization.[18] Optimized ternary PTBT-Th:IHIC-N:IHIC OSCs give PCE = 11.9%.

Molecules similar to IHIC-N (structures **I** and **II**, Figure 1) have recently been reported;[19,20] however, these differ in the solubilizing substituents (R) and in the regioisomerism of the naphthalene cores, which are 1,2,5,6-substituted (rather than the quasi-linear 2,3,6,7-substitution pattern in IHIC-N). The synthesis of both of these cores depends on the α-positions (C-1 and C-5) of naphthalenes generally being the most active toward electrophilic reactions.[21] "S"-shaped compounds of type **I** ultimately rely on the electrophilic 1,5-dibromination of 2,6-dimethylnaphthalene, while the cores of compounds of type **II** are synthesized through intramolecular Friedel−Crafts alkylation/cyclizations on to the 1,5-positions of 2,6-disubstituted naphthalenes. Our synthesis of IHIC-N relies on the availability of **1** (Figure 2), the recently reported synthesis of which requires six steps and gives an overall 16% yield.[22] We developed a much more atom-economical approach to **1** using a highly

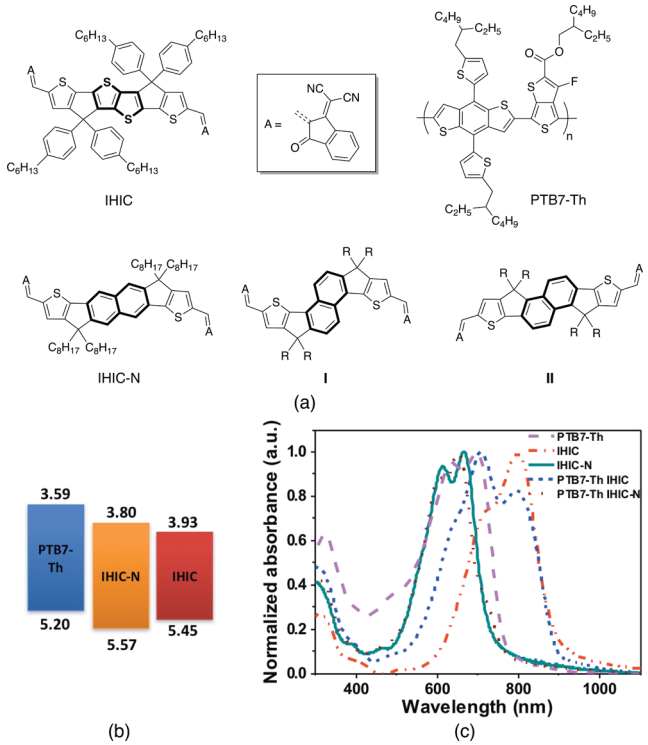

Figure 1. (a) Chemical structures of materials discussed in the text. (b) Estimated IEs and EAs for PTB7-Th, IHIC-N, and IHIC. (c) Thin-film UV−vis-NIR absorption spectra of PTB7-Th, IHIC, IHIC-N, and blends.

Received: October 26, 2017
Revised: December 19, 2017
Published: January 3, 2018

© 2018 American Chemical Society

DOI: 10.1021/acs.chemmater.7b04499
Chem. Mater. 2018, 30, 309−313

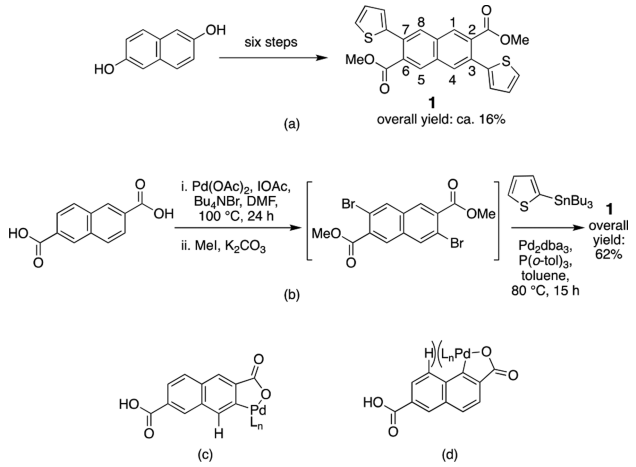

Figure 2. (a) Six-step synthesis of key intermediate **1**.[22] (b) Synthesis of **1** based on carboxylic acid-directed 3,7-dibromination and cross coupling. (c) Presumed intermediate in 3-bromination and (d) intermediate for 1-bromination, destabilized by Pd/8-hydrogen steric interactions.

regioselective double C−H functionalization of 2,6-naphthalic acid. Carboxylate-directed bromination conditions first developed by Yu[23] gave 3,7-dibromo-2,6-naphthalic acid, which was then esterified, and coupled with 2-(tributylstannyl)thiophene to give **1** in 62% overall yield. The regiochemistry of the dibromination, and therefore of **1**, was confirmed using 2D NMR methods (see Supporting Information). Bromination adjacent to the carboxylic acid is attributable to chelation to form five-membered palladacycle intermediates,[23] whereas 1,5-dibromination is presumably precluded by steric interactions of the Pd with the 4,8-hydrogen atoms (Figure 2c,d).

IHIC-N exhibits an absorption band with ε_{max} = 1.2 × 10^5 M^{-1} cm^{-1} (ca. two-thirds that of IHIC) at λ_{max} = 641 nm in $CHCl_3$ (Figure S3). The absorption maximum is similar to that for **I** (R = alkyl)[19] and is blue-shifted slightly (0.04 eV) and significantly (0.28 eV) relative to a core-alkylated IDT derivative[4] and to IHIC, respectively.[13] The blue shift vs IHIC is also seen in thin-film absorption spectra in neat films and blends with PTB7-Th (Figure 1c). This difference can be mainly attributed to disruption of the delocalization of the frontier molecular orbitals in IHIC-N, relative to those of IHIC, by the more aromatic central part of the core (Figure S5). This localization is also reflected in the frontier energy levels (Figure 1b) estimated from cyclic voltammetry (see Supporting Information), in which IHIC-N exhibits higher ionization energy (IE, by 0.13 eV) and lower EA (by 0.12 eV) than IHIC.

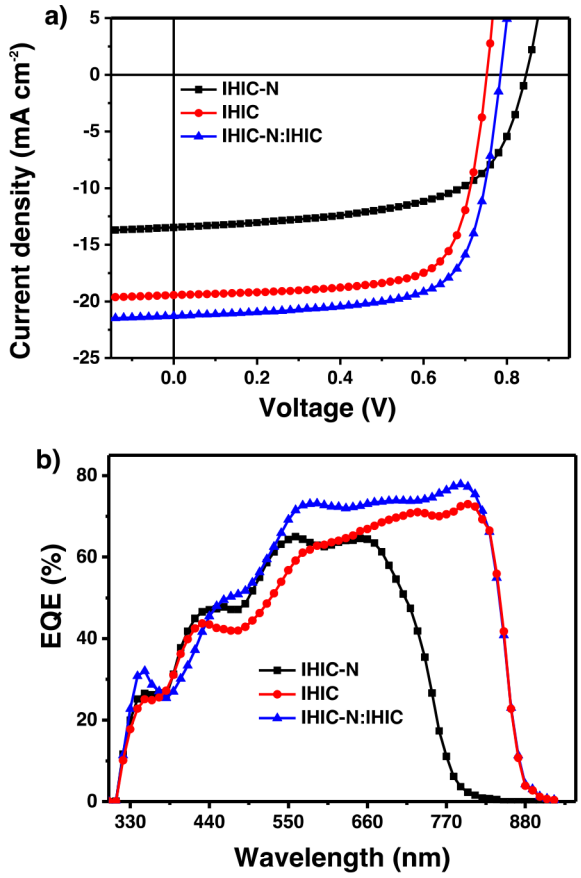

Figure 3. (a) *J*−*V* characteristics and (b) EQE spectra of the best PTB7-Th:NFA OSCs (1:1.5) under AM 1.5 G at 100 mW cm^{-2}. For the ternary cells, the IHIC-N:IHIC ratio is 1:2.

There is considerable overlap between the photoluminescence spectrum of IHIC-N and the absorption spectrum of the IHIC, indicating the possibility of energy transfer from the former to the latter (Figure S4a). The emission spectra of films of neat IHIC-N, neat IHIC, and a 1:2 w/w IHIC-N:IHIC blend, all excited at 305 nm, were also compared (Figure S4b). The emission of neat IHIC-N is relatively strong and broad (at ca. 650−850 nm) and that of IHIC (at ca. 770−850 nm) is relatively weak. The emission of IHIC-N is strongly quenched in the blend, and that of IHIC somewhat enhanced, consistent with efficient energy transfer from IHIC-N to IHIC.

ITO/ZnO/PTB7-Th:IHIC-N:IHIC/MoO_3/Ag OSCs were fabricated using a PTB7-Th:(total NFA) ratio of 1:1.5 (w/w) and varying the NFA from 100% IHIC-N to 100% IHIC (Table 1).

Table 1. Data for PTB7:Acceptor (1:1.5 w/w) OSCs with Different IHIC-N:IHIC Ratios as Acceptor[a]

Acceptor	%v/v DIO[b]	V_{OC} (mV)	J_{SC} (mA cm^{-2})	Calc. J_{SC}[c] (mA cm^{-2})	FF (%)	PCE (%)
IHIC-N	0	832 (832 ± 6)	14.1 (13.8 ± 0.4)	14.3	57.5 (56.1 ± 1.0)	6.74 (6.46 ± 0.17)
IHIC-N	0.5	846 (841 ± 3)	13.5 (13.4 ± 0.4)	13.3	60.6 (58.6 ± 1.0)	6.91 (6.59 ± 0.18)
2:1 IHIC-N:IHIC	0.5	807 (807 ± 2)	18.8 (18.8 ± 0.3)	18.0	69.3 (66.0 ± 1.7)	10.5 (10.0 ± 0.3)
1:1 IHIC-N:IHIC	0.5	787 (790 ± 5)	20.5 (20.4 ± 0.3)	19.7	68.8 (67.1 ± 1.2)	11.1 (10.9 ± 0.2)
1:2 IHIC-N:IHIC	0.5	785 (782 ± 2)	21.3 (21.2 ± 0.3)	20.3	70.8 (68.8 ± 1.2)	11.9 (11.5 ± 0.3)
1:5 IHIC-N:IHIC	0.5	781 (778 ± 4)	20.1 (19.9 ± 0.4)	19.8	70.3 (68.7 ± 1.7)	11.0 (10.6 ± 0.3)
IHIC	0.5	752 (749 ± 8)	19.4 (19.4 ± 0.3)	18.5	72.5 (70.0 ± 1.8)	10.6 (10.2 ± 0.3)

[a]Values are for the highest-PCE device, with average values and standard devices obtained from 20 devices listed in parentheses. [b]DIO = 1,8-diiodooctane. [c]Expected J_{SC} value from integration of the EQE spectra with the AM 1.5G reference spectrum; these values are within 5% of those from *J*−*V* curves.

DOI: 10.1021/acs.chemmater.7b04499
Chem. Mater. 2018, 30, 309−313

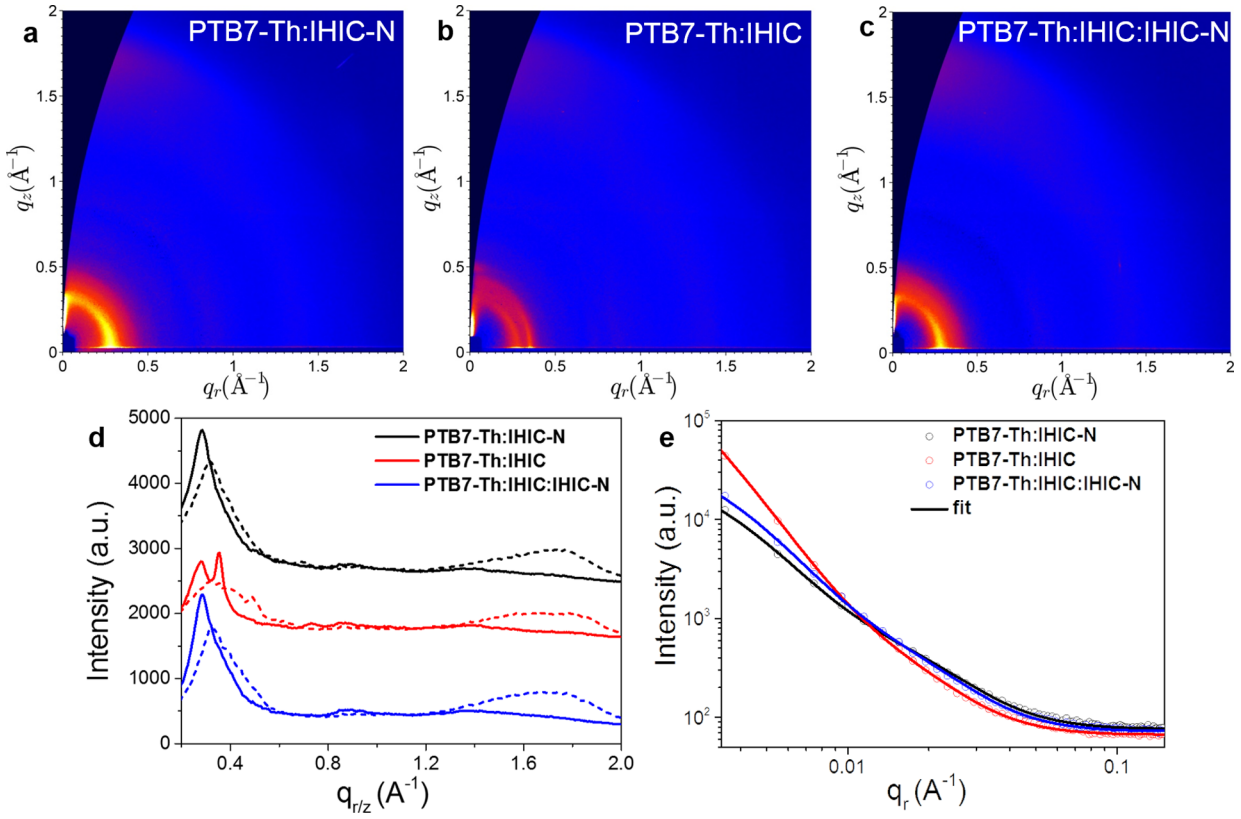

Figure 4. 2D GIWAXS patterns of (a) PTB7-Th:IHIC-N, (b) PTB7-Th:IHIC, (c) PTB7-Th:IHIC-N:IHIC (2:1:2), and (d) the corresponding GIWAXS intensity profiles along the in-plane (solid lines) and out-of-plane (dotted line) directions. (e) GISAXS intensity profiles and best fittings along the in-plane direction.

Fabrication conditions, such as additives and spin-coating speed, were optimized for PTB7-Th:IHIC-N (Table S1). 1,8-Diiodooctane (DIO) is known to improve the performance of PTB7-Th:IHIC;[24] we found it also improves PTB7-Th:IHIC-N OSCs, reducing average J_{SC}, but increasing the open-circuit voltage (V_{OC}) and fill factor (FF), resulting in slightly higher average PCE. All parameters are strongly affected by the addition of IHIC. With increasing IHIC content, average V_{OC} gradually decreases, although not in a linear fashion (Figure S7); presumably the higher EA of IHIC plays a role. The average FF generally increases. J_{SC} and PCE are both maximized at a 1:2 ratio and the PCE of 11.9% for these devices is among the highest for single-junction fullerene-free PTB7-Th OSCs (Figure 3a). However, the PCE of the ternary OSCs is relatively insensitive to the NFA composition, exceeding 11% for IHIC-N:IHIC ratios varying from 1:1 to 1:5.

EQE spectra (Figures 3b, S6, and S8) show a clear enhancement for the champion ternary device over the PTB7-Th:IHIC-N device, accounting for the improved J_{SC}; in particular, the high EQE values seen at ca. 750−850 nm are attributable to the strong NIR absorption of IHIC. The most obvious improvement in the EQE of the champion device over that of a PTB7-Th:IHIC control is at 500−700 nm, where IHIC-N absorbs. IHIC-N excitons may, in principle at least, be harvested both by electron transfer from PTB7-Th and by energy transfer to IHIC (see above), followed by electron transfer from the donor. However, the champion ternary blend also shows somewhat improved EQE at ca. 750−850 nm relative to the control, despite absorbing less strongly in this range (Figure S8).

The space-charge limited current (SCLC) method was used to measure hole and electron mobilities (μ_h and μ_e) of blend films (Figures S9 and S10; Table S2). A ternary blend (1:2 IHIC-N:IHIC) exhibited $\mu_h = 1.1 \times 10^{-3}$ cm^2 V^{-1} s^{-1}, somewhat higher than either PTB7-Th:IHIC-N (4.3×10^{-4} cm^2 V^{-1} s^{-1}) or PTB7-Th:IHIC (7.1×10^{-4} cm^2 V^{-1} s^{-1}). Values of μ_e show more variation: 2.8×10^{-5}, 1.6×10^{-3}, and 3.1×10^{-4} cm^2 V^{-1} s^{-1} for PTB7-Th:IHIC-N, PTB7-Th:IHIC, and PTB7-Th:IHIC-N:IHIC, respectively.[25] These data suggest that the ternary blends and PTB7-Th:IHIC blends both exhibit more balanced charge transport than PTB7-Th:IHIC-N blends, consistent with the much lower FF seen for the IHIC-free devices (Table 1).

GIWAXS (Figure 4a−d and S12 and GISAXS (Figures 4e and S13) were used to investigate molecular packing and nanoscale phase separation[26] in thin films of blends and neat materials. A neat IHIC-N film shows no obvious scattering peaks (Figure S13a), indicating low crystallinity, as intended by our choice of alkyl, rather than aryl, core substituents. The PTB7-Th:IHIC-N film (Figure 4a) shows a strong lamellar peak concentrated along the q_r axis (q_r = 0.284 Å^{-1}, d = 2.21 nm) and a peak attributed to π-stacking concentrated along the q_z axis (q_z = 1.73 Å^{-1}, d = 0.362 nm). These features differ somewhat from those of neat PTB7-Th for which lamellar and $\pi-\pi$ peaks are at q = ca. 0.30 and 1.60 Å^{-1}, respectively;[27] indeed, though neat PTB7-Th shows a strong feature attributed to aggregation at ca. 710 nm in its UV−vis. absorption spectrum,[28] only a weak shoulder is seen in this region for PTB7-Th:IHIC-N, also suggesting IHIC-N disrupts the polymer crystallinity. The observed $\pi-\pi$ peak might be to the scattering of IHIC-N crystalline "face-on" domains, but cannot be reliably assigned as such since neat IHIC-N exhibits poor crystallinity and so its lattice constants are unknown. The PTB7-Th:IHIC film (Figure 4b) exhibits two lamellar peaks (q_r = 0.278 and 0.354 Å^{-1}) and two $\pi-\pi$

DOI: 10.1021/acs.chemmater.7b04499
Chem. Mater. 2018, 30, 309−313

peaks (q_z = 1.60 and 1.80 Å^{-1}), suggesting that both the PTB7-Th and IHIC domains are crystalline, both with preferred "face-on" orientation. The observation of polymer scattering is consistent with the observation of the PTB7-Th aggregate peak in the absorption spectrum of the blend.[28] The π-stacking distance assigned to IHIC (0.349 nm) is somewhat smaller than that seen for the PTB7-Th:IHIC-N blend (0.362 nm). Similar broadened $\pi-\pi$ scattering features along the q_z axis are observed in the scattering pattern of the ternary PTB7-Th:IHIC-N:IHIC film, suggesting "face-on" $\pi-\pi$ stacking for both donor (PTB7-Th) and acceptor (IHIC and/or IHIC-N) materials, consistent with the more balanced carrier mobility observed in the ternary film. Figure 4e shows the GISAXS intensity profiles and best fittings along the in-plane direction. We adopted Debye−Anderson−Brumberger (DAB) and fractal-like network models to account for the scattering contribution from intermixed amorphous phases and acceptor domains, respectively.[29] The acceptor domain sizes (2Rg) are estimated to be 21.4, 22.6, and 22 nm for PTB7-Th:IHIC-N, PTB7-Th:IHIC, and PTB7-Th:IHIC-N:IHIC films, respectively, which would allow efficient exciton dissociation. The corresponding correlation lengths of the amorphous intermixed phases are fitted to be 26.9, 58.9, 27.5 nm, broadly consistent with TEM images (Figure S12), which show increasing domain size with increasing IHIC content.

In summary, we have obtained a new NFA, IHIC-N. PTB7-Th:IHIC-N:IHIC OSCs achieved PCE values of up to 11.9%, due to balanced carrier mobilities, favorable domain sizes, and broad absorption, resulting in a panchromatic photovoltaic response from 300 to 900 nm. These results also highlight the ability of C−H functionalization to access compounds that are difficult to obtain by other routes, but which are desirable to fulfill specific requirements.

■ ASSOCIATED CONTENT

Supporting Information

The Supporting Information is available free of charge on the ACS Publications website at DOI: 10.1021/acs.chemmater.7b04499.

Detailed experimental procedures and additional characterization data (solution UV−vis absorption and fluorescence spectra; electrochemical data; DFT molecular orbitals; SCLC, AFM, TEM, GIWAXS, GISAXS data; and NMR spectra) (PDF)

■ AUTHOR INFORMATION

Corresponding Authors

*xwzhan@pku.edu.cn

*seth.marder@chemistry.gatech.edu

ORCID

Stephen Barlow: 0000-0001-9059-9974

Timothy C. Parker: 0000-0002-0270-0364

Xiaowei Zhan: 0000-0002-1006-3342

Seth R. Marder: 0000-0001-6921-2536

Author Contributions

#These authors contributed equally.

Notes

The authors declare no competing financial interest.

■ ACKNOWLEDGMENTS

X.Z. thanks NSFC (No. 91433114 and 21734001); Y.X. and X.L. thank the 23A SWAXS beamline at NSRRC, Hsinchu for beam time and technical support; and J.Z., T.C.P., S.B., and S.R.M. thank NSF (CCI Center for Selective C−H Functionalization, CHE-1205646 and CHE-1700982) and ONR (N00014-14-1-0580, CAOP MURI). We thank Prof. Haoli Zhang and Xiaoting Gong from LanZhou University for the photoluminescence measurements.

■ REFERENCES

(1) Nielsen, C. B.; Holliday, S.; Chen, H. Y.; Cryer, S. J.; McCulloch, I. Non-Fullerene Electron Acceptors for Use in Organic Solar Cells. *Acc. Chem. Res.* **2015**, *48*, 2803−2812.

(2) Zhong, Y.; Trinh, M. T.; Chen, R. S.; Purdum, G. E.; Khlyabich, P. P.; Sezen, M.; Oh, S.; Zhu, H. M.; Fowler, B.; Zhang, B. Y.; Wang, W.; Nam, C. Y.; Sfeir, M. Y.; Black, C. T.; Steigerwald, M. L.; Loo, Y. L.; Ng, F.; Zhu, X. Y.; Nuckolls, C. Molecular Helices as Electron Acceptors in High-Performance Bulk Heterojunction Solar Cells. *Nat. Commun.* **2015**, *6*, 8242.

(3) Lin, Y. Z.; Zhao, F. W.; He, Q.; Huo, L. J.; Wu, Y.; Parker, T. C.; Ma, W.; Sun, Y. M.; Wang, C. R.; Zhu, D. B.; Heeger, A. J.; Marder, S. R.; Zhan, X. W. High-Performance Electron Acceptor with Thienyl Side Chains for Organic Photovoltaics. *J. Am. Chem. Soc.* **2016**, *138*, 4955−4961.

(4) Lin, Y. Z.; He, Q.; Zhao, F. W.; Huo, L. J.; Mai, J. Q.; Lu, X. H.; Su, C. J.; Li, T. F.; Wang, J. Y.; Zhu, J. S.; Sun, Y. M.; Wang, C. R.; Zhan, X. W. A Facile Planar Fused-Ring Electron Acceptor for as-Cast Polymer Solar Cells with 8.71% Efficiency. *J. Am. Chem. Soc.* **2016**, *138*, 2973−2976.

(5) Zhao, W. C.; Li, S. S.; Yao, H. F.; Zhang, S. Q.; Zhang, Y.; Yang, B.; Hou, J. H. Molecular Optimization Enables over 13% Efficiency in Organic Solar Cells. *J. Am. Chem. Soc.* **2017**, *139*, 7148−7151.

(6) Yang, Y. K.; Zhang, Z. G.; Bin, H. J.; Chen, S. S.; Gao, L.; Xue, L. W.; Yang, C.; Li, Y. F. Side-Chain Isomerization on an N-Type Organic Semiconductor Itic Acceptor Makes 11.77% High Efficiency Polymer Solar Cells. *J. Am. Chem. Soc.* **2016**, *138*, 15011−15018.

(7) Holliday, S.; Ashraf, R. S.; Wadsworth, A.; Baran, D.; Yousaf, S. A.; Nielsen, C. B.; Tan, C.-H.; Dimitrov, S. D.; Shang, Z.; Gasparini, N.; Alamoudi, M.; Laquai, F.; Brabec, C. J.; Salleo, A.; Durrant, J. R.; McCulloch, I. High-Efficiency and Air-Stable P3HT-Based Polymer Solar Cells with a New Non-Fullerene Acceptor. *Nat. Commun.* **2016**, *7*, 11585.

(8) Liu, J.; Chen, S.; Qian, D.; Gautam, B.; Yang, G.; Zhao, J.; Bergqvist, J.; Zhang, F.; Ma, W.; Ade, H.; Inganäs, O.; Gundogdu, K.; Gao, F.; Yan, H. Fast Charge Separation in a Non-Fullerene Organic Solar Cell with a Small Driving Force. *Nat. Energy* **2016**, *1*, 16089.

(9) Chen, S.; Liu, Y.; Zhang, L.; Chow, P. C. Y.; Wang, Z.; Zhang, G.; Ma, W.; Yan, H. A Wide-Bandgap Donor Polymer for Highly Efficient Non-Fullerene Organic Solar Cells with a Small Voltage Loss. *J. Am. Chem. Soc.* **2017**, *139*, 6298−6301.

(10) Lin, Y.; Zhan, X. Designing Efficient Non-Fullerene Acceptors by Tailoring Extended Fused-Rings with Electron-Deficient Groups. *Adv. Energy Mater.* **2015**, *5*, 1501063.

(11) Lin, Y. Z.; Zhao, F. W.; Wu, Y.; Chen, K.; Xia, Y. X.; Li, G. W.; Prasad, S. K. K.; Zhu, J. S.; Huo, L. J.; Bin, H. J.; Zhang, Z. G.; Guo, X.; Zhang, M. J.; Sun, Y. M.; Gao, F.; Wei, Z. X.; Ma, W.; Wang, C. R.; Hodgkiss, J.; Bo, Z. S.; Inganäs, O.; Li, Y. F.; Zhan, X. W. Mapping Polymer Donors toward High-Efficiency Fullerene Free Organic Solar Cells. *Adv. Mater.* **2017**, *29*, 1604155.

(12) Cai, Y.; Huo, L.; Sun, Y. Recent Advances in Wide-Bandgap Photovoltaic Polymers. *Adv. Mater.* **2017**, *29*, 1605437.

(13) Wang, W.; Yan, C.; Lau, T.-K.; Wang, J.; Liu, K.; Fan, Y.; Lu, X.; Zhan, X. Fused Hexacyclic Nonfullerene Acceptor with Strong near-Infrared Absorption for Semitransparent Organic Solar Cells with 9.77% Efficiency. *Adv. Mater.* **2017**, *29*, 1701308.

(14) An, Q.; Zhang, F.; Zhang, J.; Tang, W.; Deng, Z.; Hu, B. Versatile Ternary Organic Solar Cells: A Critical Review. *Energy Environ. Sci.* **2016**, *9*, 281−322.

(15) Baran, D.; Ashraf, R. S.; Hanifi, D. A.; Abdelsamie, M.; Gasparini, N.; Rohr, J. A.; Holliday, S.; Wadsworth, A.; Lockett, S.; Neophytou, M.; Emmott, C. J. M.; Nelson, J.; Brabec, C. J.; Amassian,

DOI: 10.1021/acs.chemmater.7b04499
Chem. Mater. 2018, 30, 309−313

A.; Salleo, A.; Kirchartz, T.; Durrant, J. R.; McCulloch, I. Reducing the Efficiency-Stability-Cost Gap of Organic Photovoltaics with Highly Efficient and Stable Small Molecule Acceptor Ternary Solar Cells. *Nat. Mater.* **2017**, *16*, 363−369.
(16) Yu, R.; Zhang, S.; Yao, H.; Guo, B.; Li, S.; Zhang, H.; Zhang, M.; Hou, J. Two Well-Miscible Acceptors Work as One for Efficient Fullerene-Free Organic Solar Cells. *Adv. Mater.* **2017**, *29*, 1700437.
(17) Cheng, P.; Zhan, X. Versatile Third Components for Efficient and Stable Organic Solar Cells. *Mater. Horiz.* **2015**, *2*, 462−485.
(18) Davies, H. M. L.; Du Bois, J.; Yu, J. Q. C-H Functionalization in Organic Synthesis. *Chem. Soc. Rev.* **2011**, *40*, 1855−1856.
(19) Ma, Y.; Zhang, M.; Yan, Y.; Xin, J.; Wang, T.; Ma, W.; Tang, C.; Zheng, Q. Ladder-Type Dithienonaphthalene-Based Small-Molecule Acceptors for Efficient Nonfullerene Organic Solar Cells. *Chem. Mater.* **2017**, *29*, 7942−7952.
(20) Yi, Y.-Q.-Q.; Feng, H.; Chang, M.; Zhang, H.; Wan, X.; Li, C.; Chen, Y. New Small-Molecule Acceptors Based on Hexacyclic Naphthalene(cyclopentadithiophene) for Efficient Non-Fullerene Organic Solar Cells. *J. Mater. Chem. A* **2017**, *5*, 17204−17210.
(21) Field, L. D.; Sternhell, S.; Wilton, H. V. Electrophilic Substitution in Naphthalene: Kinetic vs Thermodynamic Control. *J. Chem. Educ.* **1999**, *76*, 1246−1247.
(22) Knall, A.-C.; Ashraf, R. S.; Nikolka, M.; Nielsen, C. B.; Purushothaman, B.; Sadhanala, A.; Hurhangee, M.; Broch, K.; Harkin, D. J.; Novák, J.; Neophytou, M.; Hayoz, P.; Sirringhaus, H.; McCulloch, I. Naphthacenodithiophene Based Polymers − New Members of the Acenodithiophene Family Exhibiting High Mobility and Power Conversion Efficiency. *Adv. Funct. Mater.* **2016**, *26*, 6961−6969.
(23) Mei, T.-S.; Giri, R.; Maugel, N.; Yu, J.-Q. Pd^{II}-Catalyzed Monoselective *ortho* Halogenation of C−H Bonds Assisted by Counter Cations: A Complementary Method to Directed *ortho* Lithiation. *Angew. Chem., Int. Ed.* **2008**, *47*, 5215−5219.
(24) Zuo, L.; Yu, J.; Shi, X.; Lin, F.; Tang, W.; Jen, A. K. Y. High-Efficiency Nonfullerene Organic Solar Cells with a Parallel Tandem Configuration. *Adv. Mater.* **2017**, *29*, 1702547.
(25) μ_e for neat IHIC-N is also lower than that of neat IHIC (3.7×10^{-4} vs 2.4×10^{-3} cm^2 V^{-1} s^{-1}).
(26) Mai, J.; Lau, T.-K.; Li, J.; Peng, S.-H.; Hsu, C.-S.; Jeng, U. S.; Zeng, J.; Zhao, N.; Xiao, X.; Lu, X. Understanding Morphology Compatibility for High-Performance Ternary Organic Solar Cells. *Chem. Mater.* **2016**, *28*, 6186−6195.
(27) Bi, P.; Zheng, F.; Yang, X.; Niu, M.; Feng, L.; Qin, W.; Hao, X. Dual Förster Resonance Energy Transfer Effects in Non-Fullerene Ternary Organic Solar Cells with the Third Component Embedded in the Donor and Acceptor. *J. Mater. Chem. A* **2017**, *5*, 12120−12130.
(28) Bencheikh, F.; Duché, D.; Ruiz, C. M.; Simon, J. J.; Escoubas, L. Study of Optical Properties and Molecular Aggregation of Conjugated Low Band Gap Copolymers: PTB7 and PTB7-Th. *J. Phys. Chem. C* **2015**, *119*, 24643−24648.
(29) Mai, J.; Lu, H.; Lau, T.-K.; Peng, S.-H.; Hsu, C.-S.; Hua, W.; Zhao, N.; Xiao, X.; Lu, X. High Efficiency Ternary Organic Solar Cell with Morphology-Compatible Polymers. *J. Mater. Chem. A* **2017**, *5*, 11739−11745.

DOI: 10.1021/acs.chemmater.7b04499
Chem. Mater. 2018, 30, 309−313